International Conferences on Recent Advances in Geotechnical Earthquake Engineering and Soil Dynamics

2010 - Fifth International Conference on Recent Advances in Geotechnical Earthquake Engineering and Soil Dynamics

26 May 2010, 4:45 pm - 6:45 pm

Failure of Saturated Sand in Non-Symmetrical Cyclic Loading

J. Yang
The University of Hong Kong, Hong Kong

H. Y. Sze
The University of Hong Kong, Hong Kong

Follow this and additional works at: https://scholarsmine.mst.edu/icrageesd

Part of the Geotechnical Engineering Commons

FAILURE OF SATURATED SAND IN NON-SYMMETRICAL CYCLIC LOADING

J. Yang
The University of Hong Kong
Pokfulam Road, Hong Kong

H.Y. Sze
The University of Hong Kong
Pokfulam Road, Hong Kong

ABSTRACT

Extensive experimental studies have been focused on the cyclic behavior of saturated sand under free-field level ground conditions when subjected to earthquake loading. In many practical applications involving earth dams, slopes and buildings, however, soil elements are always subjected to initial static driving shear stresses on the horizontal planes. The impact of initial shear stresses on cyclic behavior and strength of sand is not yet fully understood. The focus of the present study is placed on the initial shear impact on the failure mechanisms of saturated sand varying from loose to dense state. Three distinctly different cyclic failure patterns have been identified. The most critical one is characterized by sudden, run-away deformation without any precautionary signal. The second failure mode is well known as cyclic mobility in which deformation takes place in double amplitude. The third type is the plastic axial strain accumulation in a single direction. It is shown that which failure pattern prevails is complicated, depending on the initial state of sand and the degree of stress reversal.

INTRODUCTION

Cyclic triaxial tests have long been utilized to study the cyclic liquefaction behavior of saturated sand under earthquake loading since the early work of Seed and Lee (1966). Over the past decades, extensive studies have been focused on isotropically consolidated sand samples under two-way, symmetrical loading in compression and extension, which represents free-field level ground conditions. In many practical applications involving earth dams, slopes and buildings, however, soil elements are subjected to an additional initial static shear stress on the horizontal planes before the earthquake loading comes into effect. To simulate this condition in triaxial tests, anisotropic consolidation of the sample is required to give rise to a static shear stress on the plane of interest in the sample. Superposition of cyclic deviator stress then produces cyclic loading that is non-symmetrical about the hydrostatic stress state.

The initial shear impact on the cyclic behavior and strength of sand is complicated and is not yet fully understood. There is only a limited number of experimental studies addressing this issue, e.g. the work of Vaid and Chern (1985), Hyodo et al. (1994) and Vaid et al. (2001). However, these test programs have focused on relatively dense sand subjected to a narrow range of initial shear levels. It is necessary to consider much higher initial shear levels since sand may behave differently when the initial shear becomes comparable with the applied cyclic shear. Also, the flow deformations showed in their

studies seemed to be limited flow with axial strain up to around 5%. It could mean the loose sand they tested was not fully contractive. The failure pattern of very loose to loose sand is certainly a subject of great interest as they are most susceptible to liquefaction.

The aim of this study is to produce comprehensive cyclic triaxial test data that can help to: (1) identify different cyclic failure patterns exhibited by saturated clean sand under various combinations of initial state and stress reversal level; (2) clarify the initial shear impact on the cyclic strength of sand under different initial states; and (3) link up the observed cyclic behavior with the resulted cyclic strength under the initial shear conditions.

EXPERIMENTATION

All cyclic triaxial tests were carried out using the CKC automated triaxial testing system (Chan, 1981). Toyoura sand, the Japanese standard sand, was employed in this investigation. It is uniform fine silica sand consisting of angular to subangular grains. Its mean grain size D_{50} is 0.216mm; coefficient of uniformity C_u is 1.39; specific gravity G_s is 2.64; maximum and minimum void ratio e_{max} and e_{min} are 0.977 and 0.605 respectively.

Moist tamping with under-compaction technique was employed aiming at creating relatively uniform samples with a wide range of void ratios. In so doing, the centermost layer was targeted at a desired relative density with each successive lower and upper layer having 1% relative density less and more, respectively. The procedure involved, first, thoroughly mixing an oven-dried batch of sand with de-aired water to achieve 5% moisture content. Secondly, the moist sand was compacted in 5 layers to achieve required density forming a specimen with 71.1mm diameter and 142.2mm height. End lubrication was provided to further ensure sample uniformity upon shearing. Thirdly, two stages of initial saturation – CO_2 flushing and de-aired water flushing were carried out as the conventional process. A further 190kPa back pressure could effectively achieve the B-value above 0.98. Full saturation of specimens is important because the soil resistance to liquefaction is sensitive to the degree of saturation (Yang, 2002; Yang et al., 2004). It is also a key factor requiring caution in dynamic physical model tests (Yang, 2004).

Another key point was to accurately control various combinations of initial state before cyclic loading. Initial confining stress and initial static shear stress levels were arrived at by anisotropic consolidation. The normal effective stress σ_{nc}' and initial static shear stress τ_s, in terms of α, on the plane of interest in the specimen were controlled by the major and minor principal consolidation pressures σ_{1c}' and σ_{3c}' as

$$\sigma_{nc}' = \frac{\sigma_{1c}' + \sigma_{3c}'}{2} \qquad (1)$$

$$\alpha = \frac{\tau_s}{\sigma_{nc}'} = \frac{\sigma_{1c}' - \sigma_{3c}'}{\sigma_{1c}' + \sigma_{3c}'} \qquad (2)$$

Finally, stress-controlled cyclic loading at 0.01Hz in sinusoidal form was applied in an undrained condition. All tests were terminated automatically or manually at excessive axial strain levels.

The test program was aimed at investigating the cyclic failure patterns and cyclic strength of sand under different combinations of initial state parameters. Toyoura sand with post-consolidation relative density D_{rc} = 10% to 70% was subjected to various levels of effective confining pressure σ_{nc}' = 100 to 500kPa, and for each confining stress level, subjected to a range of initial shear applied in triaxial compression mode up to α = 0.6. Here, only part of results is reported to illustrate the key distinctions between failure patterns as well as the initial shear impact on the cyclic strength of sand.

CYCLIC FAILURE PATTERNS

The experimental results showed that the cyclic failure patterns of moist-tamped Toyoura sand fell into three types as 1) strain softening with run-away deformation in a single direction; 2) cyclic mobility with double-amplitude cyclic

strain gain; and 3) plastic strain accumulation in a single direction. Which type of failure will occur depends on the initial state of sand and the degree of stress reversal. Generally, the initial state in terms of relative density and effective confining pressure controls the contractiveness / dilativeness of sand. The relative amplitude of initial static shear and applied cyclic shear, on the other hand, determines the degree of stress reversal.

Strain Softening

It was observed that all loose sand at D_{rc} = 10% and 20% always underwent sudden run-away deformation at failure. The general mechanism leading to this strain softening response remains the same under any consolidation stress state and any degree of stress reversal. Indeed, this strain softening response was dictated by the contractiveness of sand at its initial state.

Without Initial Shear. Figure 1 shows the undrained cyclic response of 10% Toyoura sand under σ_{nc}' = 100kPa without any initial shear. Cyclic deviator stress q_{cyc} applied at 25kPa was in complete reversal. In the course of loading, progressive buildup of pore water pressure (PWP) was observed. What corresponded was the continuous drop of soil effective stress. The axial deformation was, however, not obvious during this initial process. After 31 loading cycles, the excess PWP suddenly underwent a dramatic rise to the level of initial effective confining pressure. Sudden, excessive and irrecoverable axial strain was developed in extension up to 15%. The direction of run-away deformation was likely controlled by the greater contractiveness of sand in extension than in compression. This complete loss of shear strength and shear stiffness resulted in sample collapse as observed in Fig. 2. The redistribution of pore water and sand grains was obvious indicating entire structure collapse. The unnoticeable soil deformation before run-away deformation might lead to an impression that the soil was still very stable or at least in the way of destabilization. Thus, this sudden flow-type failure is certainly dangerous since the resulted soil deformation is abrupt and without any precautionary signal.

This strain softening response can be viewed in a more rational way through its stress path in the stress space (q – p' plane). Effective stress state kept migrating towards the critical state line (CSL), which defines the ultimate state at which soil is sheared at constant volume and constant stress. As soon as the stress state was brought to or sufficiently close to the critical stress ratio (CSR) line (Vaid and Chern, 1985), which defines the state of triggering of strain softening in monotonic loading condition, run-away deformation was initiated. Since extension CSR line has a milder slope than compression CSR line, the stress path approached the former line first, resulting in failure in extension. It corresponds to the fact that failure happened suddenly before approaching its limit at the CSL.
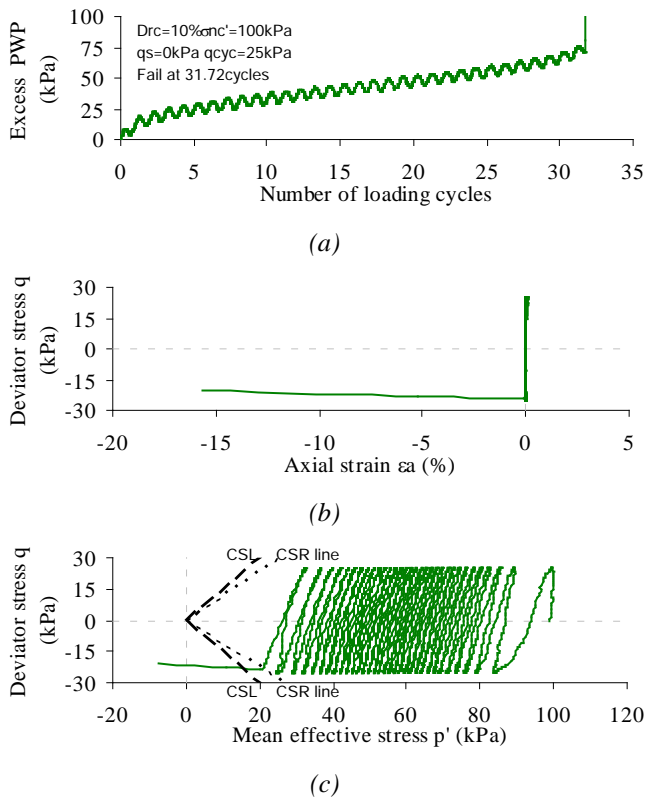
(a)

(b)

(c)

Fig. 1. Strain softening of loose sand without initial shear.

Loose sand   *Dense sand*
Fig. 2. Failure modes of loose and dense sand.

With Initial Shear. It was found that the presence of initial shear did not alter the mechanism towards strain softening but the direction of cyclic failure. Figure 3 shows how sand under previous initial state but with $\alpha = 0.4$ (i.e. the initial static deviatoric shear stress $q_s = 80$kPa) responded under a low level of $q_{cyc} = 7$kPa. Initial progressive PWP buildup and its final abrupt rise together with sudden run-away deformation were again observed. In the absence of stress reversal, cyclic loading sat entirely on the compression side. Sudden run-away deformation thus took place in compression. In the stress space, it happened when the stress path reached the compression CSR line. It is of interest to notice that sudden collapse was preceded by certain axial strain accumulation up to over 0.5%. It, however, does not mean that the occurrence of strain softening can be predicted. It is because a definite axial strain level at which run-away deformation certainly took place did not exist based on the obtained loose sand results. On the other hand, since the initial stress state was brought closer to the compression CSR line, it took less distance to approach it. That's why sudden failure took place well before the excess PWP had to elevate to its level at failure in case of $\alpha = 0$.

There exists a definite failure point which is the time when strain softening / run-away deformation is triggered. The number of cycles to reach this state was found to be around 30 cycles in both tests. The fact that a much lower level of cyclic shear was sufficient to fail the sand under $\alpha = 0.4$ reveals that the cyclic strength of loose sand decreases with initial shear level. More correctly as revealed by Yang & Sze (2008), the cyclic resistance of loose sand initially increases but then decreases with α until zero level. The phenomenon is, indeed, closely related to the distinct cyclic failure pattern exhibited by loose sand compared with that by dense sand. Details will be discussed later.
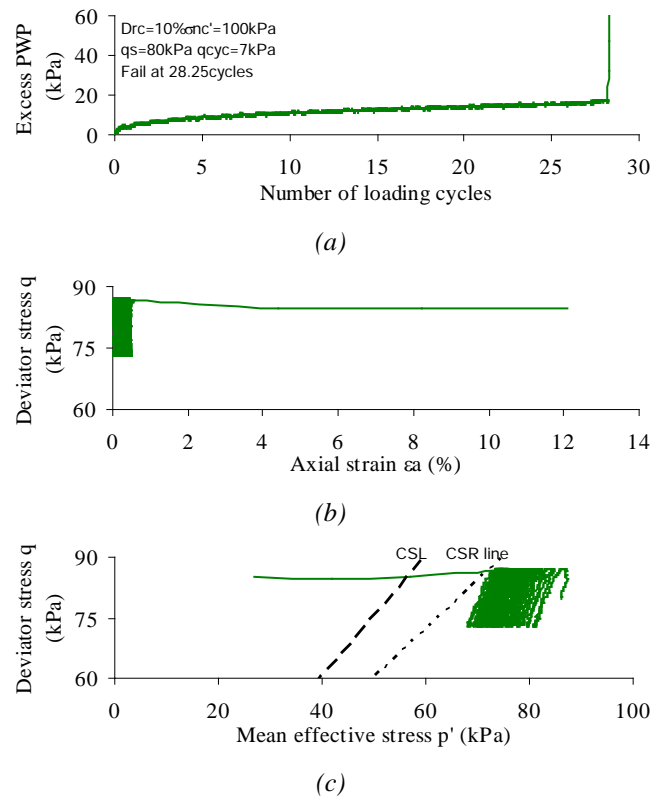

(a)

(b)

(c)

Fig. 3. Strain softening of loose sand with initial shear.

Cyclic Mobility

The cyclic failure pattern of denser sand ($D_{rc} = 50\%$ and 70%) was found very different from that of loose sand. If the stress reversal is not minimal or absent, the sample undergoes "cyclic mobility" (Castro 1975) with cyclic strain accumulation in double-amplitude (D.A.). Otherwise, plastic axial strain accumulation in a single direction will be resulted.
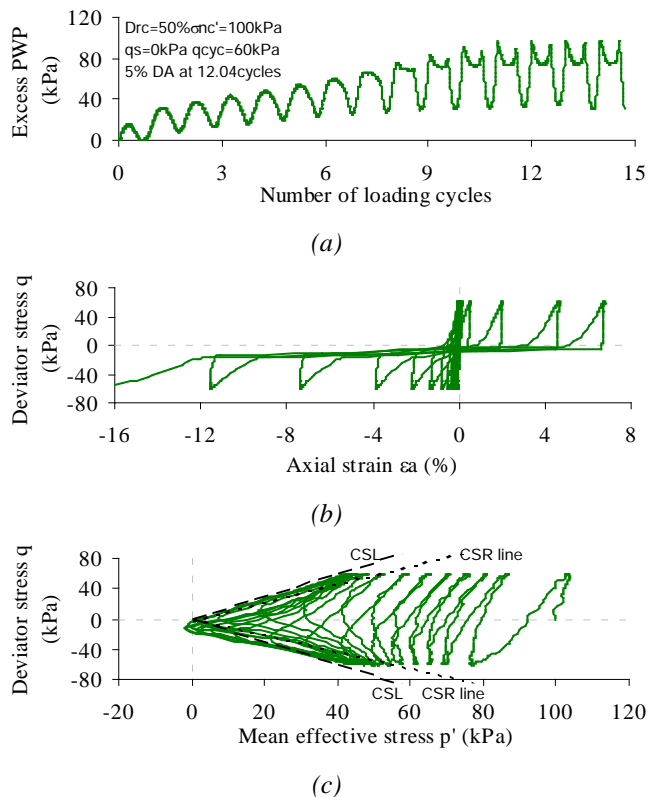
(a)

(b)

(c)

Fig. 4. Cyclic mobility of dense sand without initial shear.

Without Initial Shear. The initial mechanism leading to cyclic mobility of dense sand is actually very similar to that of loose sand. As shown in Fig. 4, the sample D_{rc} = 50% under σ_{nc}' = 100kPa was cyclically sheared without initial shear. Initially as loading proceeded, similar rise of PWP and unnoticeable soil deformation were observed. Instead of having a sudden dramatic elevation of PWP leading to the run-away deformation, the PWP buildup in dense sand was gradual all the way. One more thing to note in a particular loading cycle was the local contraction within the sand structure in a compression half-cycle and the local dilation in an extension half-cycle. It was evidenced by the local sinusoidal rise and drop of PWP. These rise and drop increased in magnitude from cycle to cycle leading to an overall PWP buildup.

As the excess PWP got close to the level of initial effective confining pressure, the progressive stiffness degradation in the sample became more obvious and a certain level of elastic axial deformation started mainly in extension. The effective stress eventually reached zero at around 10th cycle, transient softening instead of complete strain softening took place. Initial liquefaction (Seed and Lee, 1966) was said to have occurred. At almost the same instant, soil deformation increased to a magnitude hitting the compression side. Moreover, local dilation became obvious in the compression half-cycle as opposed to the local contraction observed initially. These dilations led to a regain of soil strength and stiffness during progressing cyclic disturbance. At zero

deviator stress, however, the effective stress dropped back to zero momentarily. Soil deformation also changed direction at this instant. The entire mechanism repeated itself from cycle to cycle. While the level of dilation remained almost constant in each cycle, strain gain became more and more substantial. Test terminated automatically until sample deformed over 20% D.A. with serious necking as shown in Fig. 2. The fact that strain gain was more substantial in extension evidenced the greater contractiveness of sand towards extension stress. Although this failure mode is not sudden and unnoticeable, its capability to accumulate strain up to high level under rapid shaking still imposes danger to the field.

In the stress space, progressive effective stress state migration towards the CSL was observed. CSR lines played no role here since strain softening was not probable in dense sand. Initial liquefaction was found to take place when the stress path was sufficiently close to the CSL. Since the CSL cannot be exceeded, the stress path could only approach zero effective stress at zero deviator stress. It had to follow the CSL to move away from the origin as loading continued in either compression or extension. These movements represented the local dilations observed in loading cycles after initial liquefaction; these dilations were not obvious before that. The stress path could not continue indefinitely since continuous stiffness degradation of sand under progressing cyclic disturbance resulted in unacceptably large deformations.

With Initial Shear. Similar cyclic mobility response could also be observed in the presence of high level of initial shear. It required the degree of stress reversal to be sufficiently high. Figure 5 shows an example on the same previous initial state with α = 0.4 and around 85% cyclic stress being distributed on the compression side. Some plastic axial strain accumulation was observed during early PWP buildup up to around 1% in compression. It was the result of stiffness degradation under the high compression loading imposed. Initial liquefaction took place at around 12th cycle. Cyclic mobility almost started at the same instant with elastic D.A. deformation. This deformation kept increasing afterwards and became balanced in both directions. The stress space clearly revealed that subsequent transient softening and strengthening were more substantial in compression after initial liquefaction. These were the consequences of having stress reversal dominating the compression side. Also, deformation took place early since the initial stress state was brought closer to the CSL by the very high α level.

Since softening could always be recovered by dilation, there existed no definite failure point for dense sand like the sudden run-away deformation experienced by loose sand. It then relies on the amount of D.A. strain gain and is conventionally taken as 5%. In both tests, 5% D.A. were reached at around 12 to 13 cycles. The presence of α = 0.4 required almost double cyclic stress amplitude to reach failure at the same loading cycles; this is in complete contrary to what have been observed in loose sand behavior. It is because if the cyclic stress applied is less than the initial static shear stress, dense sand will undergo

plastic strain accumulation instead. As will be observed in the followings, the resulted rate of axial strain accumulation would be much reduced and certainly cannot fulfill the specified failure criteria in significant loading cycles.
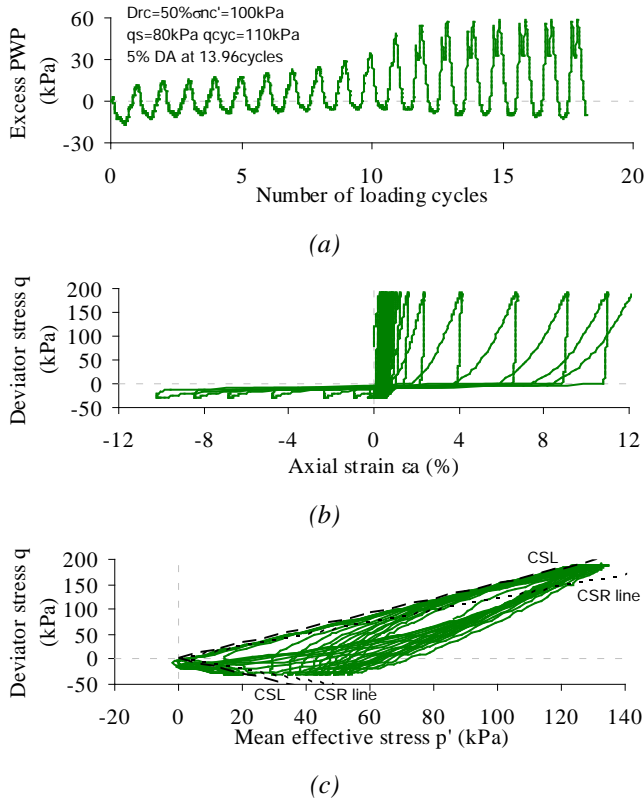

(a)

(b)

(c)

Fig. 5. Cyclic mobility of dense sand with initial shear.

Plastic Strain Accumulation

Figure 6 shows that in the presence of initial shear at $\alpha = 0.4$ under $\sigma_{nc}' = 500$kPa, the sand sample at 50% underwent plastic axial strain accumulation in compression. Stress reversal was slight in this case with only 5% distributed in extension. Although the excess PWP did keep building up, the rate was slow and in a decreasing manner. The stress path was merely looping around the compression CSL with little migration towards the origin. Since the state of $q_s + q_{cyc}$ has initially approached the critical state, soil deformation was prominent in the first cycle. After that, axial strain accumulation continued in compression but at a constant rate. Test was terminated manually when axial strain reached 9%. The fact that a high level of axial strain was being accumulated in the initial process of PWP buildup differentiates this failure mode from cyclic mobility. Also, strain gain happened only in a single direction due to the exceptionally high compression stress which, however, could not fail the sample in a flow-type manner like loose sand.

Such low level of extension stress was unable to trigger mobility in D.A. not to say if it was absent. In case without

stress reversal, the rate of plastic strain accumulation would be further reduced and was certainly not comparable with that during cyclic mobility. To ensure the failure criterion for this mode being comparable with that for cyclic mobility, 5% peak axial strain (P.S.) was chosen. It is because both criteria refer to the same level of deformation with serviceability consideration.
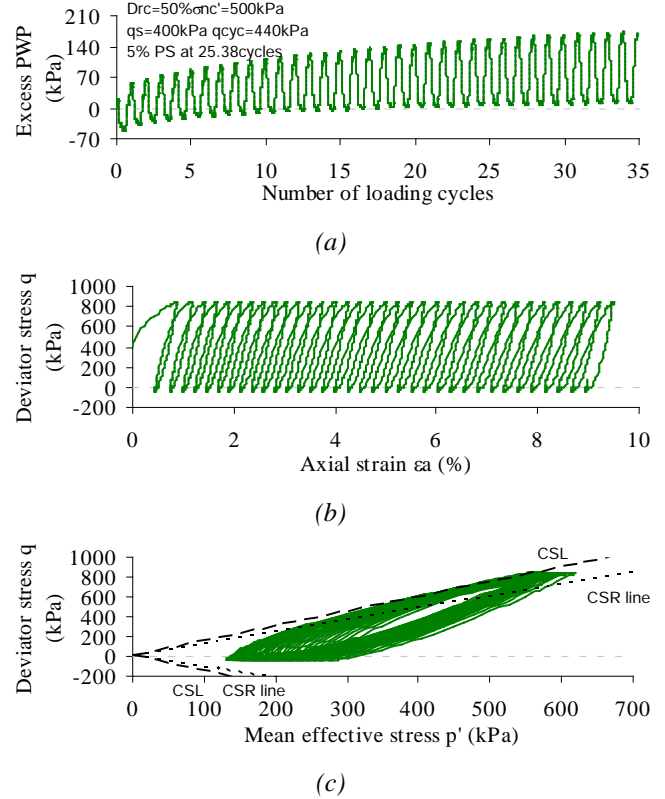

(a)

(b)

(c)

Fig. 6 Plastic strain accumulation of dense sand.

CYCLIC STRENGTH OF SAND

The cyclic strength of Toyoura sand specified at 10 loading cycles under various initial states were evaluated according to the aforementioned failure criteria for the three failure patterns. It is expressed as the cyclic resistance ratio

$$CRR_n = \frac{q_{cyc}}{2\sigma_{nc}'} = \frac{\tau_{cyc}}{\sigma_{nc}'} \tag{3}$$

where τ_{cyc} is the cyclic shear stress on the plane of interest and the subscript n denotes the use of σ_{nc}' as the denominator. It is in contrast to the conventional use of σ_{3c}' because it should be σ_{nc}' representing the in-situ overburden pressure particularly when initial shear presents. The cyclic strength so-obtained was found to be highly dependent on the three initial state parameters – relative density, effective confining pressure and initial static shear stress as shown in Fig. 7. Indeed, this dependence is closely related to the cyclic failure modes the sand exhibits.
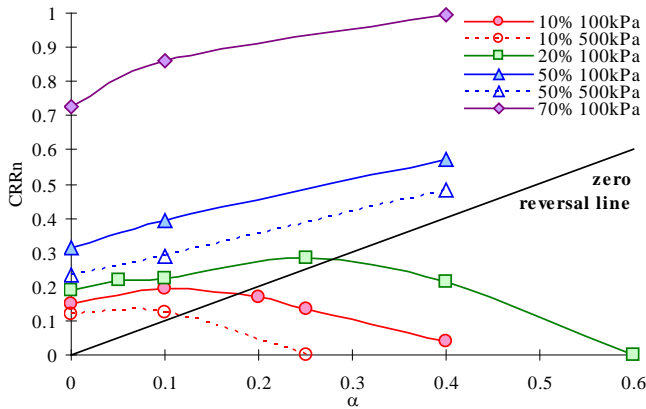
Fig. 7. Cyclic strength of Toyoura sand at different initial states under initial shear impact.

State-Dependent Nature of Cyclic Strength

Regardless of the level of initial shear, CRR_n always increases with increasing D_{rc} and / or decreasing σ_{nc}'. It means that more dilative sand bears higher cyclic strength. This is considered reasonable as cyclic liquefaction failure is the direct result of the contractive nature of sand. This observation matches the custom view but proves here to be true even under very high levels of initial shear.

Cyclic Strength of Loose Sand under Initial Shear Impact

The cyclic strength of loose sand and dense sand varies distinctly under the initial shear impact. For loose sand, there exists a clear trend that CRR_n always increases and then decreases with α. This observed rise and drop of cyclic strength rely primarily on four conditions. First, the strain softening nature of loose sand in compression is comparable with that in extension i.e. loose sand is collapsible in both compression and extension at comparable level of applied stress. Second, strain softening must happen in loose sand once either of the CSR lines is being touched. Third, in which direction run-away deformation takes place depends on which CSR line the initial stress state positions closer to. Last but not the least, the compression CSR line on the q – p' plane has a steeper slope than the extension one for a particular initial state.

With the above considerations, Fig. 8 illustrates how cyclic strength varies under initial shear impact. At $\alpha = 0$, initial stress state of sand lies on the p' axis at mean effective stress p_c' after consolidation. Since it positions closer to the extension CSR line, its stress path during undrained cyclic disturbance would hit this line first. The sample then deforms suddenly in extension.
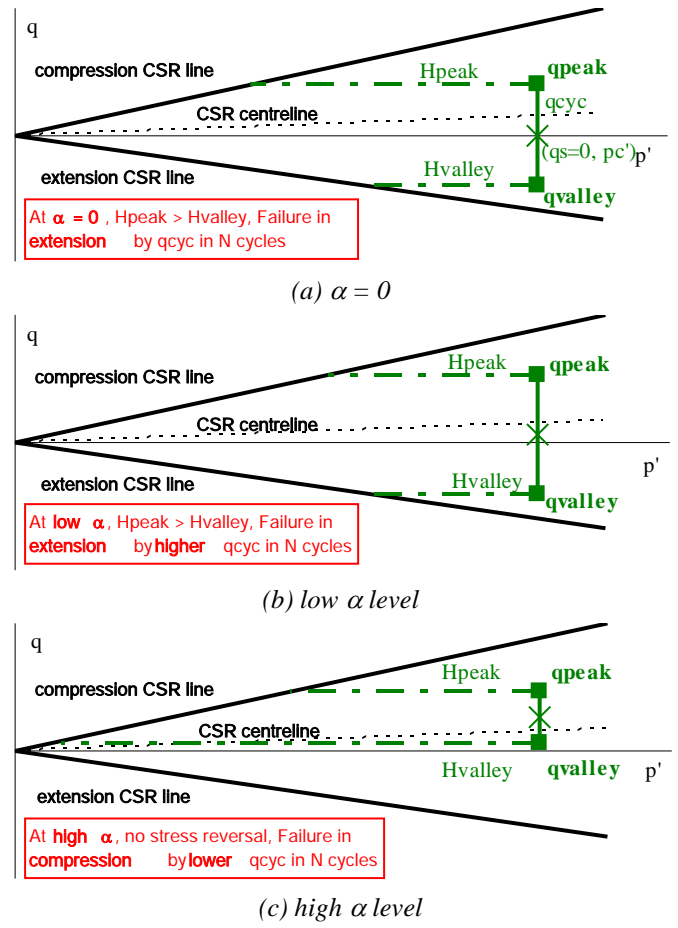

(a) $\alpha = 0$

(b) low α level

(c) high α level

Fig. 8. Variations of cyclic stress to trigger strain softening in loose sand in same loading cycles under different α levels.

For initial shear applied in triaxial compression mode, imposing static shear will bring the initial stress state onto the corresponding α line which is a straight line passing through the origin in the stress space having a constant slope depending on α such that,

$$\frac{q_s}{p_c'} = \frac{6\alpha}{3-\alpha} \qquad (4)$$

As long as the α line that it sits on is not sloping steeper than the CSR centerline between the compression and extension CSR lines, the initial state should still be closer to the extension line as shown in Fig. 8(b). In this case, cyclic stress amplitude has to be increased to yield a higher valley deviator stress q_{valley} so that the stress path can approach the extension CSR line in the same loading cycles as when $\alpha = 0$. It tells why cyclic strength increases with α at low level. Beyond this centerline, the cyclic stress amplitude does not have to increase further since strain softening can be triggered in compression. Figure 8(c) shows that much lower q_{cyc} will be enough to yield a peak deviator stress q_{peak} so that the stress path can reach the compression CSR line in the same cycles.

This illustrates the decreasing cyclic strength with initial shear at high levels.

Threshold α and Zero Reversal Line. Yang and Sze (2008) and Yang et al. (2009) proposed the concept of threshold α and zero reversal line to empirically characterize the observed beneficial and then detrimental initial shear impact on cyclic strength of loose sand. It becomes reasonable to think that this threshold α, above which CRR_n starts to drop, should correspond to the level of α whose α line in the stress space coincides with the CSR centerline. The threshold α can hence be estimated based on the critical stress ratios of sand at that certain initial state.

The zero reversal line along which $CRR_n = \alpha$ is drawn in Fig. 7. Stress reversal is always present on the left but absent on the right side of this line. Evidently, once a $CRR_n - \alpha$ trendline crosses the zero reversal line, a drop in cyclic strength commences. This drop corresponds to the absence of stress reversal, meaning that strain softening must take place in compression. This observed link between CRR_n drop and failure direction change matches the specific cyclic failure pattern exhibited by loose sand as discussed previously.

Cyclic Strength of Dense Sand under Initial Shear Impact

The cyclic resistance of dense sand, unlike loose sand, keeps increasing within the α range tested without showing any sign of drop. Again, it is the direct consequence of the failure patterns exhibited by dense sand. The cyclic strength is specified as the cyclic stress sufficient to deform the sample axially to 5% D.A. or 5% P.S. in 10 loading cycles. Experimental evidence suggests that the rate of strain accumulation in a single direction is much slower than that in double-amplitude. Thus, increasing initial shear must increase also the cyclic shear to yield enough stress reversal to trigger cyclic mobility instead of plastic strain accumulation in the same fixed loading cycles. Further increasing α may lead to a drop of CRR_n in dense sand if the trendline eventually touches the zero reversal line. This is likely to happen in the 50% sample but unlikely in the 70% sample, since such α level may not be practically attainable. It is thought that if a drop does commence, the failure pattern of dense sand under such high level of initial shear may have altered or the resulted plastic strain accumulation would become very rapid.

CONCLUSIONS

Based on a comprehensive cyclic triaxial experimental study, three distinct cyclic failure patterns of sand were identified depending on its initial state and the degree of stress reversal:

(1) Strain softening with sudden, unpredictable run-away deformation is the unique cyclic response of loose sand regardless of the initial stress states. The flow is dramatic with

over 15% axial strain development in no time. When and in what direction failure takes place are controlled by whether the compression or extension CSR line is being reached.

(2) Dense sand exhibits cyclic mobility whenever stress reversal is not minimal. Progressive stiffness degradation is associated with soil deformation in double-amplitude. Deformation keeps accumulating axially even substantial dilation reinstalls the soil strength and stiffness after initial liquefaction.

(3) With a low degree of or without stress reversal, dense sand undergoes plastic axial strain accumulation in a single direction. The rate of deformation is much slower than that during cyclic mobility but the amplitude can approach a certain high level even in the mid-way of PWP buildup.

Cyclic strength under the initial shear impact was found to be highly state dependent. Dense sand bears higher cyclic strength at increasing α level, since only higher level of cyclic shear is able to deform the sample substantially through cyclic mobility but not plastic strain accumulation. The presence of initial shear on loose sand is, however, beneficial only at low α level but detrimental at higher level. It is because the collapse strength as characterized by the CSR line of loose sand in compression is comparable with that in extension. Last but not the least, the previously suggested concept of threshold α and zero reversal line was found able to fit into the correspondences between the observed failure patterns and cyclic strength variations under the impact of the three initial state parameters.

REFERENCES

Castro, G. [1975]. "Liquefaction and Cyclic Mobility of Saturated Sands", J. of Geo. Engrg. Div., ASCE, Vol. 101, No. GT6, pp. 551-569.

Chan, C.K. [1981]. "An Electropneumatic Cyclic Loading System", Geo. Test. J., Vol. 4, No. 4, pp. 183-187.

Hyodo, M., Tanimizu, H., Yasufuku, N. and Murata, H. [1994]. "Undrained Cyclic and Monotonic Triaxial Behavior of Saturated Loose Sand", Soils and Founds., Vol. 34, No. 4, pp. 19-32.

Seed, H.B. and Lee, K.L. [1966]. "Liquefaction of Saturated Sands during Cyclic Loading", J. of Soil Mech. and Found. Div., ASCE, Vol. 92, No. SM6, pp. 105-134.

Vaid, Y.P. and Chern, J.C. [1985]. "Cyclic and Monotonic Undrained Response of Sands", *Proc. Adv. in the Art of Testing Soils under Cyclic Loading Conditions*, ASCE, Detroit, pp. 171-176.

Vaid, Y.P., Stedman, J.D. and Sivathayalan, S. [2001]. "Confining Stress and Static Shear Effects in Cyclic Liquefaction", Can. Geo. J., Vol. 38, No. 3, pp. 580-591.

Yang, J. [2002]. "Liquefaction Resistance of Sand in Relation to P-wave Velocity", Géotechnique, Vol. 52, No. 4, pp. 295-298.

Yang, J. [2004]. "Reappraisal of Vertical Motion Effects on Soil Liquefaction", Géotechnique, Vol. 54, No. 10, pp. 671-676.

Yang, J., Savidis, S. and Roemer, M. [2004]. "Evaluating Liquefaction Strength of Partially Saturated Sand", J. Geotech Geoenv. Engrg., ASCE, Vol. 130, No. 9, 975-979.

Yang, J. and Sze, H.Y. [2008]. "Undrained Cyclic Behavior of Loose sand under Anisotropic Consolidation", *Proc. 14th World Conf. on Earthquake Engrg.*, Beijing, China.
Yang, J., Sze, H.Y. and Heung, M.K. [2009]. "Effect of Static Initial Shear on Cyclic Behavior of Sand", *Proc. 17th Int. Conf. on Soil Mech. Geotech. Engrg.,* Alexandre, Egypt.